

APPLICATION OF THE WALSH TRANSFORM IN AN INTEGRATED ALGORITHM FOR THE DETECTION OF INTERICTAL SPIKES

D. Sanchez¹, M. Adjouadi¹, A. Barreto¹, P. Jayakar², I. Yaylali²

¹Electrical & Computer Engineering, Florida International University, FL, USA

²Neuroscience Center, Miami Children's Hospital, FL, USA

Abstract-This paper introduces a novel spike detection algorithm based on the use of Walsh Transforms. The algorithm focuses on the assessment of characteristics in the Electroencephalogram (EEG) signal that reveal the presence of a spike feature. The mathematical formulation of the algorithm is introduced and results obtained from the analysis of data from 7 epileptic patients are presented.

Keywords - EEG analysis, interictal spike detection, Walsh transform

I. INTRODUCTION¹

Electroencephalogram (EEG) recordings provide dynamic evidence of ongoing electrical activity in the brain. EEG is particularly useful in determining the presence, extent and origins of neurological disorders, such as epilepsy. The abnormal brain activity in between epileptic seizures, captured by the EEG as interictal spikes is frequently used as a valuable source of information towards the characterization of the patient's illness and possible courses of action. It is in this context that automated methods for the identification of these interictal spikes are of great help to the clinicians, as a helpful pre-screening tool to reduce the large volume of patient EEG data obtained from long-term monitoring, and as an objective, unbiased evaluation of the signals from the patient. This paper describes the definition of a new spike detection algorithm that uses the Walsh Transformation to assess some of the characteristics of the EEG signals and looks for a match with those characteristics that are commonly associated with interictal spike activity.

II. METHODOLOGY

Traditionally, the two characteristics that are considered as most reliable in the detection of spikes and sharp transients are the fast rise and decay of the spike, and the sharpness of its peak, which may be measured by the first and second derivatives of the signal, respectively [3, 4]. The spatio-temporal context of the EEG is also taken into account in several of the pattern recognition or rule-based systems used for spike detection [5, 8, 9].

The algorithm introduced here attempts to decorrelate the input EEG signals into orthogonal bases with different orders (degrees of sharpness) and different dimensions (degrees of fuzziness) using the Walsh transformation, in order to detect interictal spikes. The algorithm uses the transformation as a means to assess the degree in which the basic characteristics of spikes are present within a window of observation in the EEG signals.

¹ This work was sponsored by NSF Grants: EIA-9812636 and EIA-9906600, the NSF Graduate Research Fellowship of Ms. Danmary Sanchez and ONR Grant N00014-99-1-0952.

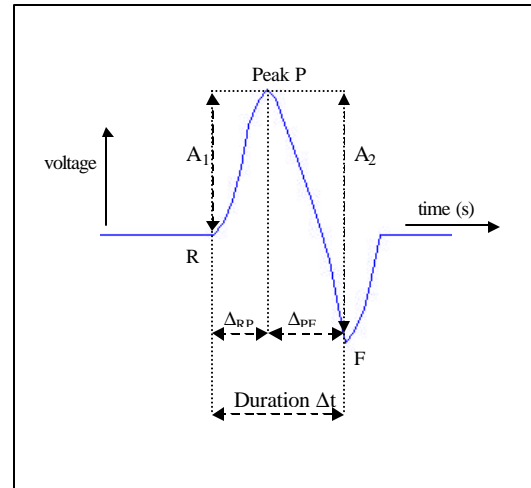


Fig. 1. Simulated spike used to describe the morphology of interictal spikes.

A. Criteria used in characterizing interictal spikes

Although interictal spikes differ greatly from one patient to the next, and even within recordings from the same patient, many spikes follow a general characterizing pattern. This general waveform is simulated in Figure 1.

As a result of the information provided by neuroscientists at Miami Children's Hospital (MCH) and our literature search in this field, the following list of primordial criteria was established, with reference to Figure 1, as necessary to declare the existence of an interictal spike:

1. The interictal spike is considered to be the waveform RPF , with two half waves RP and PF .
2. Both the rising and falling slopes of the spike are very steep.
3. The spike is characterized by a sharp peak P , which is due to a sudden change in polarity of the voltage signal recorded. This sharpness occurs in both the time domain and the spatial domain.
4. The sharpness of the spike is continuous, i.e. the spikes must "display sharpness in both narrow and wide intervals of observation" [2].

B. Algorithm Development

The Walsh Transform is a well-known orthogonal transformation with many applications in signal and image processing. The Walsh matrix is an n by n symmetric and orthogonal matrix consisting of $+1$ and -1 as its elements to constitute square waveforms as its basis functions [6]. The matrix obtained from the Walsh transformation kernel may be expanded to any dimension $N = 2^n$.

Report Documentation Page

Report Date 25 Oct 2001	Report Type N/A	Dates Covered (from... to) -
Title and Subtitle Application of the Walsh Transform in An Integrated Algorithm for the Detection of Interictal Spikes	Contract Number	
	Grant Number	
	Program Element Number	
Author(s)	Project Number	
	Task Number	
	Work Unit Number	
Performing Organization Name(s) and Address(es) Electrical & Computer Engineering Florida International University , FL	Performing Organization Report Number	
Sponsoring/Monitoring Agency Name(s) and Address(es) US Army Research, Development & Standardization Group PSC 802 Box 15 FPO AE 09499-1500	Sponsor/Monitor's Acronym(s)	
	Sponsor/Monitor's Report Number(s)	
Distribution/Availability Statement Approved for public release, distribution unlimited		
Supplementary Notes Papers from 23rd Annual International Conference of the IEEE Engineering in Medicine and Biology Society, October 25-28, 2001, held in Istanbul, Turkey. See also ADM001351 for entire conference on cd-rom., The original document contains color images.		
Abstract		
Subject Terms		
Report Classification unclassified	Classification of this page unclassified	
Classification of Abstract unclassified	Limitation of Abstract UU	
Number of Pages 4		

For the ordered Walsh kernel matrix, the Walsh operator \mathbf{W}_N^r of r^{th} order and length N is defined based on the sequency value and dimension N considered. The order r is given by the sequency of the vector, and refers to the type of differentiation used between sample points. The dimension N refers to the degree of fuzziness in this type of differentiation. Considering the time dependent input signal $f(t)$, the Walsh transformation W_N^r is given by the convolution of \mathbf{W}_N^r and $f(t)$ as:

$$W_N^r = \mathbf{W}_N^r * f(t) \quad (1)$$

If we consider the Walsh operator of 1st order and length 2, \mathbf{W}_2^1 , we realize that it is equal to the discrete mathematical 1st derivative, d^1 , which can be thought of as the differences between adjacent sampled points:

$$\mathbf{w}_2^1 = [1 \ -1] = d^1 \quad (2)$$

On the other hand, if we consider the Walsh operator of 2nd order and length 4, \mathbf{W}_4^2 , we realize that it is not equal, but equivalent, to the discrete mathematical 2nd derivative, d^2 , which can be thought of as the difference between two 2-point differences of three adjacent points, or the difference between two contiguous first derivatives:

$$\mathbf{w}_4^2 = [1 \ -1 \ -1 \ 1] \cong d^2 = [1 \ -2 \ 1] \quad (3)$$

At this point, we can make the generalization that \mathbf{W}_N^1 is equivalent to d^1 , and \mathbf{W}_N^2 is equivalent to d^2 (in the sense noted above) for any length N , with N being the degree of fuzziness in the differentiation. This equivalency means that they perform the same operation when convolved with the input signal, but they take into account different number of points from the input signal, depending on the length N . In other words, with a larger N , the degree of fuzziness of these derivatives is larger, and thus different characteristics of the input signal may be appreciated. With this generalization we may also say that the Walsh operators \mathbf{W}_N^1 and \mathbf{W}_N^2 may be used as operators for the first and second derivatives, respectively, with advantages noted in the orthogonality of the vectors and in the simplicity of their computation [1].

After further analysis of the behavior of W_N^r in relation to typical, bi-phasic interictal spikes, we were able to establish the following observations: (1) The results from W_N^1 yield two peaks for each spike. The first peak is associated with the rising-side slope, and the second peak is associated with the falling-side slope. The amplitude of each peak in W_N^1 is an indicator of the steepness of the slope, where a higher peak means a steeper slope. (2) The results from W_N^2 yield a peak associated to the peak location of the spike. The amplitude of this peak in W_N^2 is an indicator of the sharpness of the apex of the spike, where a higher peak means a sharper apex.

In order to extract an interictal spike from the background signal, we developed a set of integrated mathematical expressions based on the Walsh operators. Criterion 4 defined in the previous section states that an interictal spike must

exhibit continuous sharpness. In other words, it must be sharp in narrow as well as in wider intervals of observation. This implies that an actual interictal spike must result in high values for the peaks in W_N^1 and W_N^2 for several lengths N .

To analyze that required multi-scale sharpness, we consider the outputs of these Walsh operators but using different scales by means of the different lengths of the operators W_N^1 and W_N^2 . In this case we use $N = 4, 8, \text{ and } 16$ as the number of points analyzed in the input data. This type of approach was also used in a study by Barreto [2] for the detection of interictal spikes in ECoG, but using Lagrange derivatives to measure the EEG sharpness.

In order to account for several intervals of observation, the algorithm we developed takes the results at different scales and then adds them together to detect the presence of sharpness under different scaling. This is expressed mathematically as:

$$\mathcal{W}^r = W_4^r + W_8^r + W_{16}^r \quad (4)$$

for $r = 1, 2$. The motivation in this operation is to extract all potential transitions using different scales for assessing sharpness, in an additive way. In other words, if sharpness of the signal is identified in any of W_4^r , W_8^r , or W_{16}^r , resulting in high-amplitude peaks, this will yield the recognition of a sharp signal in \mathcal{W}^r as well.

On the other hand, actual interictal spikes must also exhibit high local sharpness. The best way to measure this is through the convolution of the actual mathematical first and second derivatives, with the time signal $f(t)$ as:

$$D^1 = d^1 * f(t) \text{ and } D^2 = d^2 * f(t) \quad (5)$$

which take into account only 2 and 3 data points of the input signal, respectively.

Since the interictal spike must exhibit high degrees of sharpness in both the narrow and wider intervals, we need to combine the resulting measures of sharpness in both intervals. This is achieved with a point-by-point multiplication between the actual mathematical derivative, given by D^r , and the addition of the Walsh transformations of different length N , given by $W_4^r + W_8^r + W_{16}^r$. Therefore, the term \mathcal{W}^r becomes a function of the derivatives and of the Walsh transformation, as:

$$\mathcal{W}^r(D^r, W_N^r) = D^r \cdot [W_4^r + W_8^r + W_{16}^r] \quad (6)$$

for $r = 1, 2$. So, individually, these functions for orders 1 and 2 will be described as:

$$\begin{aligned} \text{(a) } \mathcal{W}^1 &= D^1 \cdot (W_4^1 + W_8^1 + W_{16}^1), \text{ and} \\ \text{(b) } \mathcal{W}^2 &= D^2 \cdot (W_4^2 + W_8^2 + W_{16}^2) \end{aligned} \quad (7)$$

The objective of this point-to-point product is to selectively reinforce the parts of the signal that resulted in large outputs

from the derivative (D) and composite Walsh ($W_4 + W_8 + W_{16}$) transforms.

By observing the responses of the Walsh transformations, we noted that at points where an interictal spike is defined, two prominent peaks occur in W^1 , delimiting the duration of the spikes, and one prominent peak occurs in W^2 , corresponding to the sharp apex of the spike.

After applying these mathematical expressions to the epileptogenic EEG from different patients, we confirmed that the results in W^r emphasize the presence of a signal that meets both of the main characteristics of the interictal spike: sustained steep slopes and sharp peak. At this point, dynamic thresholds were set in order to eliminate the W^r responses of low amplitude in both the temporal and spatial domains. The thresholds were set to be dynamic to take into consideration the variations in amplitude and frequency of the background activity.

The dynamic threshold was set equal to twice the standard deviation about the mean, calculated for the signals in the local background. For the temporal dynamic threshold, we defined the local background activity to be a time window with duration of 3 seconds. In Figure 2 (a), we display a 5 second EEG block collected at channels P₃ through T₆. Note that there is an interictal spike identified in electrode F₈. In Figure 2 (b), the W^r signal obtained for the EEG in channel F₈ is displayed, as well as the W^r signal obtained after the dynamic temporal threshold has been applied. If we apply the dynamic temporal threshold to all of the EEG channels shown in Figure 2 (a), we obtain the plots in Figure 2 (c) for the W^1 signals. It may be observed in these plots that, when comparing the peaks in W^1 for every electrode at the time instance where the spike is identified (almost 0.5 seconds into the segment), the highest peaks are those seen in F₈, which is precisely the location of the spike. This observation allows for the implementation of the dynamic spatial threshold, calculated across all electrodes at each specific instant of time. In Figure 2 (d), the signals obtained as a result of applying the spatial threshold are displayed again for all channels. We can see here that those peaks that were smaller than the background across the rest of the electrodes have already been eliminated.

In order to refine the detection of spikes from these dynamic thresholds, a set of mathematical rules were applied to the W^r signal in order to confirm the presence of the rest of the criteria that identify interictal spikes. These included checks for (1) total duration of the interictal spike or sharp wave to be from 20 to 200 milli-seconds, (2) amplitude of the spike to be above 20 micro-volts, (3) ratio of amplitude between the spike and the background activity to be greater than 1.6, and (4) reduction of artifacts such as EKG and background signal, among others. All of these checks were performed with the use of the W^r signal, as opposed to the EEG signal itself.

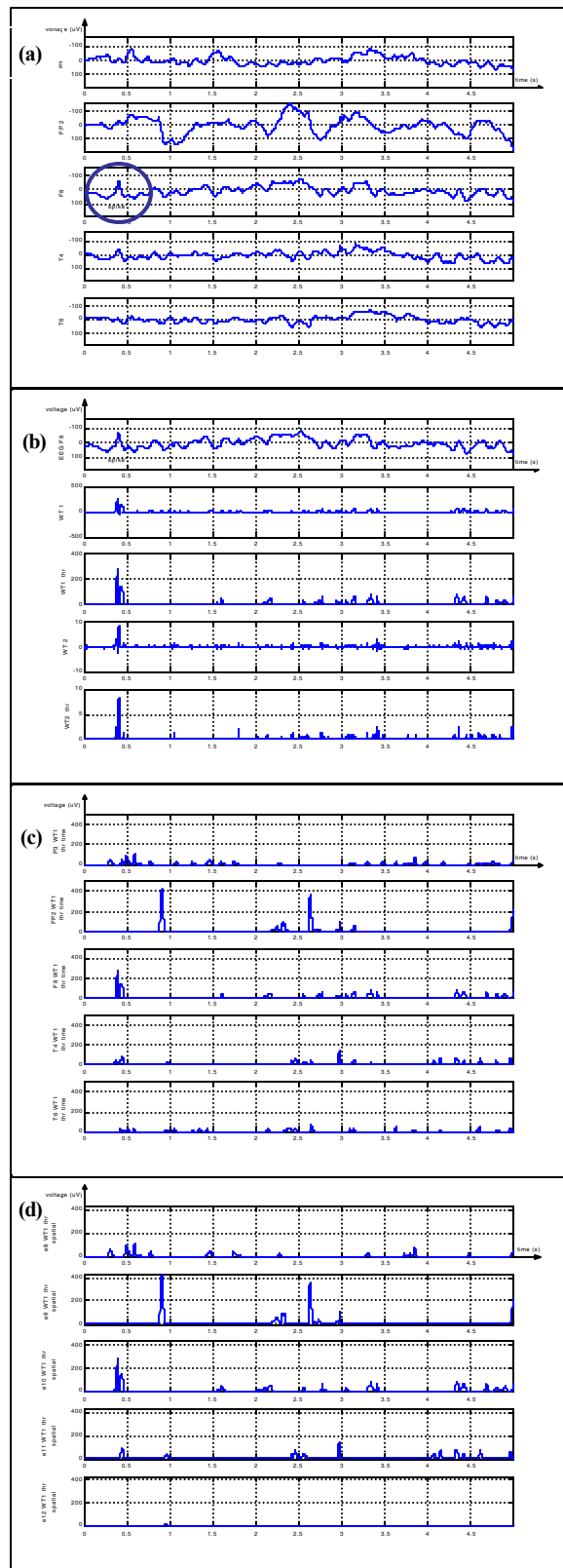


Fig. 2. Sample EEG segment processed by the algorithm. (a) EEG signals P3 through T6. (b) Calculation of the W^r on the F8 signal and application of the temporal dynamic threshold. (c) Temporal dynamic thresholds for all channels. (d) Spatial dynamic threshold for all channels.

III. RESULTS

A. System Evaluation Setup

The efficiency of the proposed interictal spike detection algorithm was tested with EEG data recorded from 7 patients at Miami Children's Hospital, using the 10-20 Electrode System and a sampling rate of 500 samples/second, per channel. The 21 channel signals were recorded with respect to a reference electrode located close to the vertex. A NeuroScan Electrical Signal Imaging system, and the associated recording software were used to capture EEG from the patients in digital files. About 20 minutes of EEG from each patient were used for the evaluation of the algorithm.

B. Evaluation Parameters and Results

Prior to any processing by the proposed algorithm, two human experts, a clinical neuroscientist and a registered EEG technologist, scored the files electronically, upon review in the NeuroScan system. Each of them, independently, marked all instances of interictal spikes they found in the files. For the initial assessment of the algorithm, a spike was acknowledged as a true event if at least one of the experts had marked it. There were a total of $TOT_SPK = 163$ such spikes. After running the same files through the algorithm, the system identifications that matched the events found by either human expert were considered true positives (TP), and the rest were considered false positives (FP). Events marked by at least one expert, but not detected by the algorithm were identified as false negatives (FN). With these counts the sensitivity (TP/TOT_SPK) and the precision ($TP / (TP + FP)$) for the algorithm were calculated. They are shown in Table I.

Table I. Performance of the spike detection algorithm
(Note: Spikes acknowledged if marked by either expert)

Set	Sensitivity	Precision
All 7 patients	$108/163$ $=0.66$	$108/(108 + 91)$ $=0.54$

IV. DISCUSSION

The results summarized in Table I are encouraging, particularly when we consider that this level of performance was obtained from direct analysis of the EEG signals themselves, within a short window of observation, and without reference to global considerations, such as the state of the subject, or other contextual clues.

It should also be kept in mind that the sensitivity of the system, as reported in Table I, uses the broadest criterion for the acceptance of a true interictal event (at least one expert found it). If we were to apply a more stringent criterion, such that only events marked as spikes by both experts are accepted, then the sensitivity of the system with respect to this new "golden standard" would be much higher, approaching 89%.

The algorithm also proved to be robust against the detection of a number of biologically-generated artifacts, such as those induced by talking, jaw movement, muscle movement, eye blinking, eye movement, coughing, and swallowing. These were recorded from a non-epileptic subject, and successfully ignored by the algorithm.

V. CONCLUSION

The primary characterizing features of interictal spikes, enumerated in this paper, were embedded in our system for the extraction of the spikes from the background activity. We translated each of these characteristics into a mathematical formula such that we could implement them in the development of our algorithm. The spike detection algorithm developed through this study was based on the Walsh transformation, which is an orthogonal transformation that decomposes the signal into mutually independent constituents, each of which can be useful in the overall interpretation process of the EEG. Encouraging results were obtained from the application of the algorithm to EEG data from seven patients.

REFERENCES

- [1] Adjouadi, M., Candocia, F., "A stereo matching paradigm based on the Walsh Transformation," IEEE Trans. on Pattern Analysis and Machine Intelligence, 16(12): 1212–1218, 1994.
- [2] Barreto, A. B., A Spatio-Temporal Approach to Epileptic Focus Localization From Array Electroencephalography, University of Florida, Gainesville, FL, 1993.
- [3] Birkemeier, W. P., Fontaine, A. B., Celesia, G. G., Ma, K. M., "Pattern Recognition Techniques for the Detection of Epileptic Transients in EEG," IEEE Transactions on Biomedical Engineering, BME-25(3): 213–217, 1978.
- [4] Davey, B. L. K., Fright, W. R., Carroll, G. J., Jones, R. D., "Expert System Approach to Detection of Epileptiform Activity in the EEG," Medical and Biological Engineering and Computing, 27: 365–370, 1989.
- [5] Glover, J. R., Raghavan, N., Ktonas, P. Y., Frost, J. D., "Context-Based Automated Detection of Epileptogenic Sharp Transients in the EEG: Elimination of False Positives," IEEE Transactions on Biomedical Engineering, 36: 519–527, 1989.
- [6] Gonzalez, R. C., Woods, R. E., "Image Transforms," Digital Image Processing, Addison-Wesley Publishing Co., 81–159, 1993.
- [7] Gotman, J., "Practical Use Of Computer- Assisted EEG Interpretation In Epilepsy," Clinical Neurophysiology, 2(3): 251–265, 1985.
- [8] Gotman, J., Wang, L. Y., "State Dependent Spike Detection: Validation," Electroencephalography and Clinical Neurophysiology, 83: 12–18, 1992.
- [9] Jayakar, P., Patrick, J. P., Shweddyk, E., Seshia, S. S., "Automated Rule Based Graded Analysis Of Ambulatory Cassette EEGs," Electroenceph. Clin. Neurophysiol., 72: 165–175, 1989.